Biochem. J. (2013) **456**, 361–372 (Printed in Great Britain) doi:10.1042/BJ20130486

A TFG–TEC nuclear localization mutant forms complexes with the wild-type TFG–TEC oncoprotein and suppresses its activity

Bobae LIM*[1], Ah-young KIM*[1], Hee Jung JUN* and Jungho KIM*[2]

*Laboratory of Molecular and Cellular Biology, Department of Life Sciences, Sogang University, Seoul 121-742, South Korea

Human EMCs (extraskeletal myxoid chondrosarcomas) are soft tissue tumours characterized by specific chromosomal abnormalities. Recently, a proportion of EMCs were found to harbour a characteristic translocation, t(3;9)(q11-12;q22), involving the *TFG* (TRK-fused gene) at 3q11-12 and the *TEC* (translocated in extraskeletal chondrosarcoma) gene at 9q22. The present study used both *in vitro* and *in vivo* systems to show that the TFG–TEC protein self-associates, and that this is dependent upon the CC (coiled-coil) domain (amino acids 97–124), the AF1 (activation function 1) domain (amino acids 275–562) and the DBD (DNA-binding domain) (amino acids 563–655). The TFG–TEC protein also associated with a mutant NLS-TFG–TEC (AAAA) protein, which harbours mutations in the NLS (nuclear localization signal). Subcellular localization assays showed that the NLS mutant TFG–TEC (AAAA) protein interfered with the nuclear localization of wild-type TFG–TEC. Most importantly, the mutant protein inhibited TFG–TEC-mediated transcriptional activation *in vivo*. Thus mutations in the *TFG–TEC* NLS yield a dominant-negative protein. These results show that the biological functions of the *TFG-TEC* oncogene can be modulated by a dominant-negative mutant.

Key words: chromosomal translocation, dominant-negative, fusion protein, human extraskeletal myxoid chondrosarcoma, nuclear localization mutant, TFG–TEC.

INTRODUCTION

Recurrent chromosome translocations are the hallmark of many human cancers, including human EMCs (extraskeletal myxoid chondrosarcomas). Human EMCs are rare soft tissue tumours of uncertain differentiation, with an uncertain histogenetic origin (although they arise primarily in the musculature, most commonly the thigh and knee) [1–3]. Most human EMCs harbour characteristic translocations, either t(9;22)(q22;q12) or t(9;17)(q22;q11.2), which involve the *TEC* (translocated in extraskeletal chondrosarcoma) gene at 9q22, and either the *EWS* (Ewing's sarcoma) gene at 22q12 or the *hTAF$_{II}$68* (human TATA-binding protein-associated factor II 68) gene at 17q11.2 [1,3–6]. Another translocation, t(9;15)(q22;q21), has also been reported, resulting in a *TCF12* (transcription factor 12)-*TEC* fusion gene in human EMCs [7], although this is much less common.

Recently, a proportion of human EMCs was found to harbour a characteristic translocation, t(3;9)(q11-12;q22), involving the *TFG* (TRK-fused gene) at 3q11-12 and the *TEC* gene at 9q22 [8]. *TFG* was originally identified as a fusion partner for the *NTRK1* (neurotrophic tyrosine kinase receptor type 1) gene in human papillary thyroid carcinoma [9], and is also involved in another chromosome translocation [involving the *ALK* (anaplastic lymphoma receptor tyrosine kinase) gene] in anaplastic large-cell lymphomas [10]. *TFG* is located on the q arm of human chromosome 3 and encodes a ubiquitously expressed cytoplasmic protein [9]. The complete *TFG* cDNA comprises 1677 bp and encodes a protein of 400 amino acids, containing putative functional domains, including the PB1 (Phox and Bem1p) domain, a CC (coiled-coil) domain and a SPYGQ (serine, proline, tyrosine, glycine and glutamine)-rich region [11]. The TFG protein interacts with the NEMO [NF-κB (nuclear factor κB) essential modulator] and TANK [TRAF (tumour-necrosis-factor-receptor-associated factor)-associated NF-κB activator] proteins, suggesting that it may play a key role in NF-κB regulation [12]. Interestingly, primary structure analysis of the TFG protein reveals multiple myristylation sites, indicating that it may localize to the cell membrane [11]. However, the biological role of the *TFG* gene in normal cells is largely unknown.

TEC is the human homologue of rat *Nor-1* (neuron-derived orphan receptor 1) [13], and is also known as *CHN* [1] and *MINOR* [14]. It was first isolated from primary cultures of apoptotic rat forebrain neurons [13] and encodes a novel orphan nuclear receptor belonging to the steroid/thyroid receptor gene superfamily [1,3]. It was also identified as a fusion partner for the *EWS* gene in human EMCs [3]. The *TEC* gene is located at 9q22 [15], spans ~40 kb, and contains eight exons, of which exons 1 and 2 correspond to the 5′-untranslated sequence of the mature *TEC* mRNA [15]. Although the biological role of *TEC* remains unknown, reports indicate that the constitutive expression of *TEC* induces massive cell death in thymocytes [16], suggesting that it may play a role in cell proliferation by regulating its downstream target genes.

The present study shows that the *TFG-TEC* oncogene product can self-associate, and that the responsible regions map to the CC (amino acids 97–124), AF1 (activation function 1; amino acids 275–562) and DBD (DNA-binding domain) (amino acids 563-655) regions. Mutations in the TFG–TEC NLS (nuclear localization signal) ($K^{612}RRR^{615}$) yielded a protein that was unable to localize to the nucleus, but was still able to associate

Abbreviations used: AF, activation function; CC, coiled-coil; DBD, DNA-binding domain; EMC, extraskeletal myxoid chondrosarcoma; Eno3, enolase 3; EWS, Ewing's sarcoma; HEK, human embryonic kidney; HPRT, hypoxanthine–guanine phosphoribosyltransferase; hTAF$_{II}$68, human TATA-binding protein-associated factor II 68; LBD, ligand-binding domain; NBRE, nerve growth factor IB-response element; NF-κB, nuclear factor κB; NLS, nuclear localization signal; NTD, N-terminal domain; PB1, Phox and Bem1p; RT, reverse transcription; Stat3, signal transducer and activator of transcription 3; Socs2, suppressor of cytokine signalling 2; TEC, translocated in extraskeletal chondrosarcoma; TFG, TRK-fused gene; TLS, translated in liposarcoma.

[1] These authors contributed equally to the study.

[2] To whom correspondence should be addressed (email jkim@sogang.ac.kr).

with wild-type TFG–TEC. Interestingly, the NLS mutant TFG–TEC (AAAA) protein interfered with the nuclear localization of wild-type TFG–TEC. In addition, co-expression of the NLS mutant TFG–TEC (AAAA) *in vivo* inhibited TFG–TEC-mediated transcriptional activation, suggesting that it acts in a dominant-negative manner. Taken together, these data suggest that the biological activity of TFG–TEC can be modulated by the NLS mutant TFG–TEC (AAAA) protein. Because the *TFG-TEC* gene is thought to play a critical role in the formation of some human EMCs by modulating the transcription of specific TEC target genes required for tumorigenesis, the results of the present study may help to identify new therapeutic targets for the treatment of human EMCs harbouring the TFG–TEC fusion.

MATERIALS AND METHODS

Materials and general methods

Restriction endonucleases, calf intestinal alkaline phosphatase, the Klenow fragment of DNA polymerase I and T4 DNA ligase were purchased from New England Biolabs. PfuTurbo polymerase was purchased from Stratagene, and [γ-^{32}P]ATP (3000 Ci/mmol) was obtained from PerkinElmer Life Sciences. The preparation of plasmid DNA, restriction enzyme digestion, agarose gel electrophoresis, DNA ligation, bacterial transformations and SDS/PAGE were performed using standard methods [17]. Sub-clones generated from the PCR products were sequenced using the chain termination method and double-stranded DNA templates to ensure the absence of mutations.

Constructs

The plasmid pEF-BOS/GST has been described previously [18]. To generate pEF-BOS/GST-TFG-TEC, pCMV-Tag2A/TFG-TEC [19] was digested with NotI and the digested fragment was cloned into the same site of pEF-BOS/GST. To construct pcDNA4-HisMaxA/TFG-TEC, pCMV-Tag2A/TFG-TEC was digested with NotI and the digested fragment was cloned into the same site of pcDNA4-HisMaxA (Invitrogen). To generate pcDNA4-HisMaxA/TFG (NTD), pCMV-Tag2A/TFG (NTD) [19] was digested with NotI and the digested fragment was cloned into the same site of pcDNA4-HisMaxA. To construct pcDNA4-HisMaxA/TEC, pCMV-Tag2A/TEC [20] was digested with NotI and the digested fragment was cloned into the same site of pcDNA4-HisMaxA. To construct pcDNA4-HisMaxA/TFG-TEC (AAAA), pCMV-Tag2A/TFG-TEC (AAAA) was digested with XhoI, and the XhoI(AAAA)XhoI fragment was isolated. This fragment was cloned then into the same site of pcDNA4-HisMaxA/TFG-TEC to introduce the (KRRR◇AAAA) mutation into the NLS.

The GST–TFG–TEC deletion mutants were generated as follows. (i) GST–TFG [NTD (N-terminal domain)]: the TFG (NTD) fragment was amplified from pCMV-Tag2A/TFG-TEC by PCR using the primers 5′-TFGTEC_aa1_BamHI (5′-GATCGGATCCATGAACGGACAGTTGGAT-3′, BamHI site underlined) and 3′-TFGTEC_aa274_NotI (5′-GATCGCGGCCGCTCAATCTGAATACTGAATACC-3′, NotI site underlined), digested with BamHI and NotI, and cloned into the corresponding sites of the pGEX (4T-1) vector (GE Healthcare) to generate GST–TFG (NTD). (ii) GST–TEC: the TEC fragment was amplified from pCMV-Tag2A/TFG-TEC by PCR using the primers 5′-TFGTEC_aa275_BamHI (5′-GATCGGATCCATGCCCTGCGTCCAAGCC-3′, BamHI site underlined) and 3′-TFGTEC_aa900_NotI (5′-GATCGCGGCCGCTTAGAAAGGTAGGGTGTC-3′, NotI site underlined), digested with BamHI and NotI, and cloned into the corresponding sites of the pGEX (4T-1) vector to generate GST–TEC. (iii) GST–PB1: the PB1 fragment was amplified from pCMV-Tag2A/TFG-TEC by PCR using the primers 5′-TFGTEC_PB1_BamHI (5′-GATCGGATCCATGAACGGACAGTTGGAT-3′, BamHI site underlined) and 3′-TFGTEC_PB1_NotI (5′-GATCGCGGCCGCTCAGGGTCTTGGCTGGCCATT-3′, NotI site underlined), digested with BamHI and NotI, and cloned into the corresponding sites of pGEX (4T-1) to generate GST–PB1. (iv) GST–CC: the CC fragment was amplified from pCMV-Tag2A/TFG-TEC by PCR using the primers 5′-TFGTEC_CC_BamHI (5′-GATCGGATCCCTTGAATCAAGTCAGGTG-3′, BamHI site underlined) and 3′-TFGTEC_CC_NotI (5′-GATCGCGGCCGCTTCCAAGCTATCCAATAA-3′, NotI site underlined), digested with BamHI and NotI, and cloned into the corresponding sites of pGEX (4T-1) to generate GST-CC. (v) GST–SPYGQ: the SPYGQ fragment was amplified from pCMV-Tag2A/TFG-TEC by PCR using the primers 5′-TFGTEC_SPYGQ_BamHI (5′-GATCGGATCCCCACCTGGAGAACCAGGA-3′, BamHI site underlined) and 3′-TFGTEC_SPYGQ_NotI (5′-GATCGCGGCCGCTCAATCTGAATACTGAATACC-3′, NotI site underlined), digested with BamHI and NotI, and cloned into the corresponding sites of pGEX (4T-1) to generate GST–SPYGQ. (vi) GST–AF1: the AF1 fragment was amplified from pCMV-Tag2A/TFG-TEC by PCR using the primers 5′-TFGTEC_AF1_BamHI (5′-GATCGGATCCATGCCCTGCGTCCAAGCC-3′, BamHI site underlined) and 3′-TFGTEC_AF1_NotI (5′-GATCGCGGCCGCTCAGCCAGACGACGAGCTCCT-3′, NotI site underlined), digested with BamHI and NotI, and cloned into the corresponding sites of pGEX (4T-1) to generate GST–AF1. (vii) GST–DBD: the DBD fragment was amplified from pCMV-Tag2A/TFG-TEC by PCR using the primers 5′-TFGTEC_DBD_BamHI (5′-GATCGGATCCGAGGGCACGTGTGCCGTG-3′, BamHI site underlined) and 3′-TFGTEC_DBD_NotI (5′-GATCGCGGCCGCTCATGGGCTCTTTGGTTTGGA-3′, NotI site underlined), digested with BamHI and NotI, and cloned into the corresponding sites of pGEX (4T-1) to generate GST–DBD. (viii) GST–LBD (ligand-binding domain): the LBD fragment was amplified from pCMV-Tag2A/TFG-TEC by PCR using the primers 5′-TFGTEC_LBD_BamHI (5′-GATCGGATCCTTACAACAGGAACCTTCT-3′, BamHI site underlined) and 3′-TFGTEC_LBD_NotI (5′-GATCGCGGCCGCTCAAGACACCAAGTCTTCCAG-3′, NotI site underlined), digested with BamHI and NotI, and cloned into the corresponding sites of pGEX (4T-1) to generate GST–LBD. (ix) GST–AF2: a double-stranded oligomeric AF2 DNA fragment was generated by annealing using the following primer pairs: 5′-TFGTEC_AF2 (5′-pGATCCCCACCTTCCATCATTGACAAGCTCTTCCTGGACACCCTACCTTTCTAAGC-3′) and 3′-TFGTEC_AF2 (5′-pGGCCGCTTAGAAAGGTAGGGTGTCCAGGAAGAGCTTGTCAATGATGGAAGGTGGG-3′). The AF2 DNA fragment was then inserted into the BamHI/NotI sites of the pGEX (4T-1) vector to generate GST–AF2. (x) GST–DBD (AAAA): the DBD (AAAA) fragment was amplified from pcDNA4-HisMaxA/TFG-TEC (AAAA) by PCR using the primers 5′-TFGTEC_DBD_BamHI and 3′-TFGTEC_DBD_NotI, digested with BamHI and NotI, and cloned into the corresponding sites of pGEX (4T-1) to generate GST–DBD (AAAA).

The plasmids pcDNA3/EGFP and pcDNA3/EGFP-TFG-TEC have been described previously [19]. To generate pcDNA3-mCherry, an mCherry gene was PCR-amplified from pmCherry-N1 (Clontech), using primers 5-HindIIImCherry (5′-GATCAAGCTTATGGTGAGCAAGGGCGAG-3′; HindIII site underlined) and 3′-BamHImCherry (5′-GATCGGATCCGCTTACTTGTACAGCTCGTC-3′, BamHI site underlined). The PCR

product was then digested with HindIII and BamHI and cloned into the same sites in pcDNA3 to generate pcDNA3-mCherry. To construct pcDNA3/mCherry-TFG-TEC, an mCherry (NoStop) fragment was PCR-amplified from pmCherry-N1 using primers 5′-HindIIImCherry and 3′-BamHImCherry(NoStop) (5′-GATCGGATCCGCCTTGTACAGCTCGTC-3′; BamHI site underlined). The PCR product was then digested with HindIII and BamHI and cloned into the same sites in pcDNA3 to generate pcDNA3-mCherry(NoStop). pcDNA4-HisMaxA/TFG-TEC (AAAA) was digested with BamHI and NotI to isolate the TFG–TEC (AAAA) fragment, which was then cloned into the corresponding site in pcDNA3-mCherry(NoStop) to generate pcDNA3/mCherry-TFG-TEC (AAAA). To construct pcDNA4-HisMaxB/TFG-TEC, pCMV-Tag2A/TFG-TEC was digested with BamHI and the digested fragment was cloned into the same site of pcDNA4-HisMaxB (Invitrogen).

Purification of GST-fusion proteins, GST pull-down assays and Western blot analysis

GST–TFG–TEC mutant proteins were expressed in *Escherichia coli* as described previously [21]. After binding to glutathione–Sepharose and washing, the proteins were eluted with reduced glutathione (Sigma). Protein concentrations were determined using the Bio-Rad protein assay, which is based on the Bradford method. The purity and size of the eluted proteins were evaluated by Coomassie Blue staining of SDS/PAGE gels. GST pull-down assays were performed as described previously [22]. Western blot analysis was performed using anti-GST (B-14, Santa Cruz Biotechnology) or anti-Xpress (Invitrogen) antibodies, and reactive bands were detected by chemiluminescence using Western Lightening (PerkinElmer Life Sciences).

Cell culture and subcellular localization studies

HEK (human embryonic kidney)-293T cells and human C28/I2 juvenile costal chondrocyte cells (provided by Dr M. Goldring, Hospital for Special Surgery, Cornell Medical College, New York, NY U.S.A.) were maintained in DMEM (Dulbecco's modified Eagle's medium), supplemented with 10% heat-inactivated bovine serum (Gibco), penicillin and streptomycin. For the subcellular localization experiments, cells were plated on glass coverslips and transfected with the pcDNA3/EGFP-TFG-TEC or/and pcDNA3/mCherry-TFG-TEC plasmids using either the VivaMagic Reagent (Vivagen) for HEK-293T cells, or the PolyExpress Transfection Reagent (Excellgen) for C28/I2 cells. At 48 h after transfection, the cells were washed in PBS and fixed in acetone/methanol (1:1, v/v) for 10 min at $-20\,^{\circ}C$. The subcellular distribution of wild-type TFG–TEC or the NLS mutant TFG–TEC (AAAA) protein was examined under a confocal laser-scanning microscope (Leica TCS SPE, Leica Microsystems).

Reporter gene assays

Cells were transiently transfected with plasmids using the VivaMagic or PolyExpress Transfection Reagents and luciferase assays were performed using the Dual-luciferase Assay System (Promega). *Renilla* luciferase activity was used to normalize the transfection efficiency.

RT (reverse transcription)–PCR and quantitative real-time PCR

EGFP-positive and mCherry-positive transfected cells were isolated by FACS. Total RNAs were extracted from FACS-isolated population of HEK-293T and C28/I2 cells using TRIzol® reagent (Life Technologies) in accordance with the manufacturer's protocol. The RNAs were reverse-transcribed with an oligo(dT) primer using the SuperScript First-strand Synthesis System for RT–PCR (Life Technologies) to generate the first-strand cDNAs, followed by PCR to detect the expression of *Stat3* (signal transducer and activator of transcription 3), *Eno3* (enolase 3), *Socs2* (suppressor of cytokine signalling 2) and β-actin. The PCR primer sequences were: 5′-TTGCCAGTTGTGGTGATC-3′ and 5′-AGAACCCAGAAGGAGAAGC-3′ for *Stat3*; 5′-GAAGAAGGCCTGCAACTGT-3′ and 5′-ACTTGCGTCCAGCAAAGATT-3′ for *Eno3*; 5′-CTCGGTCAGACAGGATGGTA-3′ and 5′-ACAGAGATGCTGCAGAGATG-3′ for *Socs2*; and 5′- GCTCGTCGTCGACAACGGCTC-3′ and 5′- CAAACATGATCTGGGTCATCTTCTC-3′ for β-actin. The reaction products were separated on 2% agarose gels and stained with ethidium bromide.

Quantitative real-time PCR was performed using an Applied Biosystems 7500 Fast real-time PCR system and SYBR Green Master Mix (Applied Biosystems) according to the manufacturer's instructions. As a control, the level of *HPRT* (hypoxanthine–guanine phosphoribosyltransferase) mRNA was determined by quantitative real-time PCR of each RNA sample and used to correct for experimental variation. The following primer sequences were used: 5′-GCCCCGTACCTGAAGACCA-3′ and 5′-GACATCGGCAGGTCAATGG-3′ for *Stat3*; 5′-GAAGAAGGCCTGCAACTGT-3′ and 5′-ACTTGCGTCCAGCAAAGATT-3′ for *Eno3*; 5′-GGATGGTACTGGGGAAGTATGACTG-3′ and 5′-AGTCGATCAGATGAACCACACTCTC-3′ for *Socs2*; and 5′-GGACCCCACGAAGTGTTGG-3′ and 5′-CTGGCGATGTCAATAGGACTCCAG-3′ for *HPRT*. The relative expression levels of the downstream target genes were quantified by normalizing against endogenous *HPRT* using the ΔC_T method.

RESULTS

TFG–TEC can self-associate *in vivo*

The chimaeric TFG–TEC protein comprises 900 amino acids, which form seven major functional domains (Figure 1A). Three functionally important domains, the PB1 domain (residues 10–91), a CC domain (residues 97–124) and a SPYGQ-rich domain (residues 125–273) are located at the N-terminus of the TFG–TEC fusion protein. The C-terminal portion of TFG–TEC contains an AF1 transactivation domain (residues 275–562), a DBD (residues 563–655), a LBD (residues 656–885) and the AF2 transactivation domain (residues 886–900).

As shown in Figure 1(A), several functionally important domains, which are required for transcriptional modulation or protein–protein interactions, are present in the TFG–TEC protein; however, it is not clear whether TFG–TEC can self-associate. To determine whether the TFG–TEC protein could self-associate *in vivo*, we transfected HEK-293T cells with an expression vector that drives the synthesis of TFG–TEC and then performed co-affinity precipitation assays (Figure 1B). The HEK-293T cell line was chosen because TFG–TEC-positive human EMC cell lines, or their equivalents, were unavailable. HEK-293T cells were co-transfected with mammalian expression vectors containing TFG–TEC fused to GST (pEF-BOS/GST-TFG-TEC), the GST domain alone (pEF-BOS/GST) or pcDNA4-HisMaxA/TFG-TEC (which generated an N-terminal His_6-tagged and Xpress epitope-tagged TFG–TEC protein). The cells were harvested 48 h after transfection, were lysed and then incubated with glutathione beads. Immunoblotting of the eluates with the anti-Xpress antibody revealed that His_6–TFG–TEC co-precipitated with

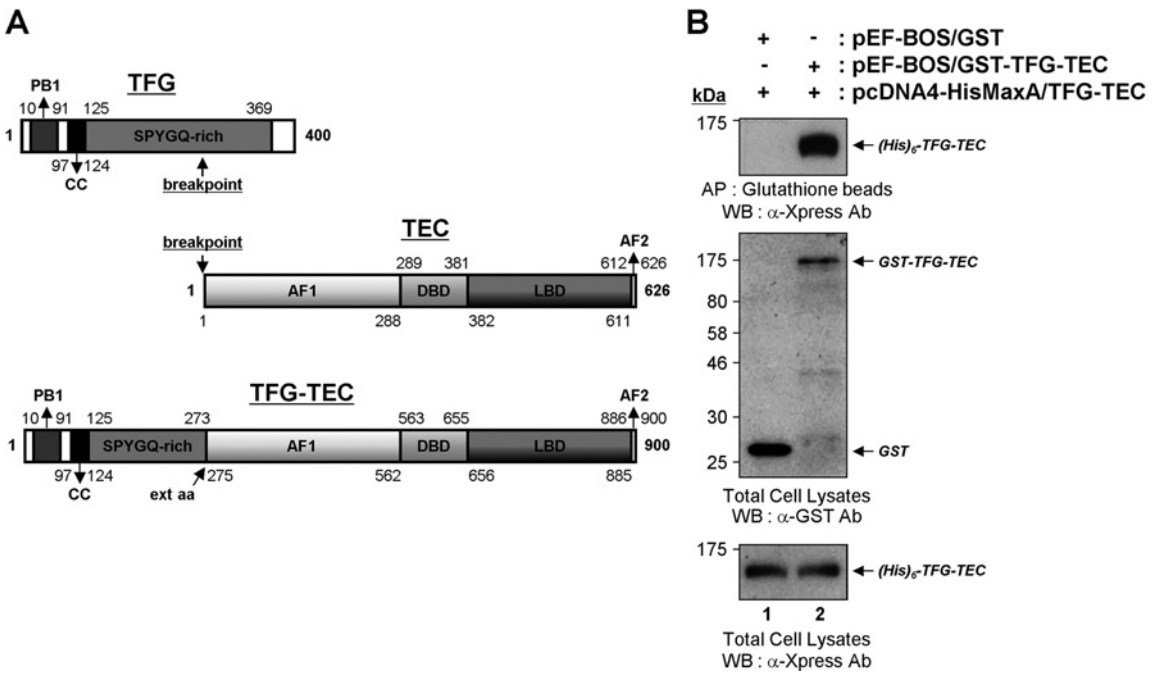

Figure 1 Self-association of TFG–TEC

(**A**) Schematic diagram illustrating the protein domains of TFG, TEC and TFG–TEC gene products. The TFG, TEC and TFG–TEC proteins are represented schematically. Amino acid positions are indicated above and below. The functionally important domains within the TFG, TEC and TFG–TEC chimaera are indicated: AF1, N-terminal transactivation domain; AF2, C-terminal transactivation domain; ext aa, extra amino acid sequence. (**B**) Self-association of TFG–TEC *in vivo*. At 48 h after transfection of HEK-293T cells with 2.5 μg of pcDNA4-HisMaxA/TFG-TEC (His_6- and Xpress epitope-tagged TFG–TEC) and 2.5 μg of either pEF-BOS/GST or pEF-BOS/GST-TFG-TEC, cell extracts were prepared as described in the Materials and methods section and affinity-precipitated with glutathione–Sepharose beads. After separation by SDS/PAGE (12 % gels), the proteins were Western blotted with an anti-Xpress or an anti-GST antibody. The identities of the transfected DNAs are shown above the panel. The positions of the molecular mass markers are indicated to the left-hand side in kDa, and the positions of His_6-tagged TFG–TEC, GST and GST-tagged TFG–TEC are indicated by the arrows on the right-hand side. Three independent experiments gave similar results. AP, affinity precipitation; Ab, antibody; WB, Western blotting.

GST–TFG–TEC, but not with GST alone (Figure 1B, top panel). The three proteins were identified in transfected cells by probing for GST (GST–TFG–TEC and GST; Figure 1B, middle panel) or the Xpress epitope (His_6–TFG–TEC; Figure 1B, bottom panel). These results demonstrated that TFG–TEC can self-associate *in vivo*.

The CC, AF1 and DBD domains of TFG–TEC are involved in self-association

To identify the domain(s) within TFG–TEC that are responsible for self-association, we performed *in vitro* pull-down assays using the GST-fusion TFG (NTD) and GST-fusion TEC proteins (Figure 2A). The TFG (NTD) and TEC fragments of TFG–TEC were generated by PCR and fused in-frame to the GST domain. These GST-fusion proteins were then expressed individually in *E. coli*, purified, and coupled to glutathione–Sepharose beads. After incubation with recombinant His_6 and Xpress epitope-tagged TFG–TEC proteins followed by extensive washing, we found that the TFG–TEC protein specifically associated with the GST fusions containing either the TFG (NTD) or TEC domains (Figure 2A; top panel, lanes 3 and 4). By contrast, there was no interaction between TFG–TEC and GST alone (Figure 2A; top panel, lane 2). These results suggest that TFG–TEC contains at least two sites [TFG (NTD) and the TEC domain] that can self-associate independently with TFG–TEC.

On the basis of these results, it was necessary to elucidate which fragment of TFG–TEC [TFG (NTD) or TEC] was involved in the interactions with TFG (NTD) and TEC. To investigate this, we expressed recombinant TFG (NTD) as a His_6-containing fusion protein in *E. coli,* and purified it using a Ni-NTA (Ni^{2+}-nitrilotriacetate)–agarose resin. A GST pull-down assay was then performed using recombinant His_6–TFG (NTD) with GST or the GST–TFG (NTD) or GST–TEC fusions. As shown in Figure 2(A, middle panel), His_6–TFG (NTD) interacted with GST–TFG (NTD), but not with GST–TEC or GST alone, indicating that TFG (NTD) interacts with TFG fragment of the TFG–TEC fusion and not with the TEC fragment.

To identify the domains(s) within TFG–TEC that are responsible for the interaction with TEC, further GST pull-down assays were performed using the His_6–TEC protein. As shown in Figure 2(A, bottom panel), the GST-fusion protein containing the TEC fragment of the TFG–TEC fusion was able to bind the His_6–TEC protein. However, the GST-fusion with TFG (NTD) failed to bind His_6–TEC (Figure 2A; bottom panel, lane 3). These results suggest that the self-association of TFG–TEC can be mediated either through the TFG (NTD) fragment or the TEC fragment of TFG–TEC. Aliquots of the GST-fusion proteins used in this assay were fractionated on SDS/PAGE (12 % gels) and visualized by Coomassie Blue staining to confirm that similar amounts of protein had been used in each pull-down assay (Figure 2B).

To identify the domain(s) within TFG (NTD) that are required for self-association, we performed *in vitro* GST pull-down assays using a series of TFG (NTD) deletion mutants. The

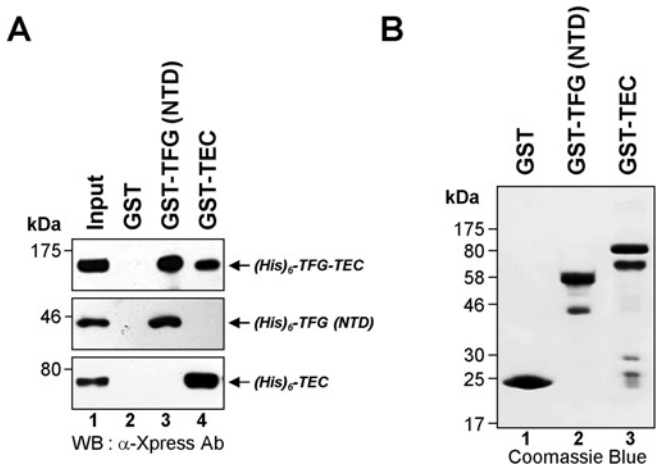

Figure 2 Binding of TFG–TEC to TFG (NTD) and TEC *in vitro*

(**A**) Two independent domains within TFG–TEC are responsible for self-association. pcDNA4-HisMaxA/TFG-TEC (top panel), pcDNA4-HisMaxA/TFG (NTD) (middle panel) or pcDNA4-HisMaxA/TEC (bottom panel) plasmid DNAs were transfected into HEK-293T cells, and cell lysates containing recombinant His_6-tagged TFG–TEC, His_6-tagged TFG (NTD) or His_6-tagged TEC proteins were incubated with 2 μg of GST (lane 2), GST–TFG (NTD) (lane 3) or GST–TEC (lane 4) respectively bound to glutathione–Sepharose beads. Aliquots of the input (2 %; lane 1) and the pellets (lanes 2–4) obtained from the GST pull-down assay were analysed on 8 % (for His_6–TFG–TEC and His_6–TEC) or 12 % [for His_6–TFG (NTD)] SDS/PAGE gels, and the bound proteins were detected by Western blotting with an anti-Xpress antibody. The positions of the molecular mass markers in kDa, His_6–TFG–TEC, His_6–TFG (NTD) and His_6–TEC are indicated. Three independent experiments were performed, all of which gave similar results. Ab, antibody; WB, Western blotting. (**B**) Quantification of the GST-fusion proteins used in the GST pull-down assays. The GST-fusion proteins utilized in the pull-down assays were fractionated on SDS/PAGE (12 % gels) and visualized by Coomassie Blue staining. Three independent experiments were performed, all of which gave similar results.

structures of the mutants are shown schematically in Figure 3(A). Figure 3(B) shows that TFG (NTD) strongly bound to GST–CC (Figure 3B; top panel, lane 4); however, the GST-fusions with PB1 (Figure 3B; top panel, lane 3) and SPYGQ (Figure 3B; top panel, lane 5) and GST alone (Figure 3B; top panel, lane 2) failed to bind, indicating that residues 97–124 of TFG–TEC are necessary and sufficient for the interaction with TFG (NTD). Aliquots of the GST-fusion proteins used in this assay were separated on SDS/PAGE (12 % gels) and visualized by Coomassie Blue staining to confirm that similar amounts of protein were used in each pull-down assay (Figure 3B; bottom panel).

We next identified the domain(s) within TEC that are required for self-association using *in vitro* GST pull-down assays and a set of TEC deletion mutants: GST–AF1, GST–DBD, GST–LBD and GST–AF2. The structures of the mutants are shown schematically in Figure 3(A). Figure 3(C) shows that His_6-tagged TEC bound strongly to GST–AF1 (Figure 3C; top panel, lane 3) and GST–DBD (Figure 3C; top panel, lane 4); however, the GST fusions with LBD (Figure 3C; top panel, lane 5) and AF2 (Figure 3C top panel, lane 6), and GST alone (Figure 3C; top panel, lane 2), failed to bind. This indicates that the AF1 or DBD domains of TFG–TEC are necessary and sufficient for the interaction with TEC. Aliquots of the GST-fusion proteins used in this assay were separated on SDS/PAGE (12 % gels) and visualized by Coomassie Blue staining to confirm that similar amounts of protein were used in each pull-down assay (Figure 3C; bottom panel). Overall, these results suggest that TFG–TEC contains at least three domains (CC, AF1 and DBD), which can self-associate independently with TFG–TEC.

The NLS mutant TFG–TEC (AAAA) protein associates with wild-type TFG–TEC *in vivo*

We previously reported that the KRRR sequence within the DBD targets the TFG–TEC oncoprotein to the nucleus [19]. To determine whether the NLS mutant TFG–TEC (AAAA) protein interacts with TFG–TEC *in vivo*, we performed co-affinity precipitations using extracts of HEK-293T cells transfected with an expression vector containing the NLS mutant TFG–TEC (AAAA) protein (Figure 4A). Site-directed mutagenesis was used to generate amino acid changes aimed at affecting the nuclear localization of TFG–TEC. Specifically, mutations were introduced into the highly conserved basic amino sequence, $K^{612}RRR^{615}$, within the DBD (which is predicted to function as a NLS for TFG–TEC) [19]; these amino acids were mutated to $A^{612}AAA^{615}$ (Figure 4A). To investigate whether the TFG–TEC mutant protein [TFG–TEC (AAAA)] associated with wild-type TFG–TEC, we transiently transfected HEK-293T cells with expression vectors containing both proteins and then performed affinity precipitation assays. HEK-293T cells were co-transfected with pcDNA4-HisMaxA/TFG-TEC (AAAA) and pEF-BOS/GST-TFG-TEC or pEF-BOS/GST. The cells were lysed 48 h after transfection and the GST–TFG–TEC fusion protein was affinity-precipitated with glutathione–Sepharose beads. Immunoblotting was then performed using the anti-Xpress antibody to detect the NLS mutant His_6–TFG–TEC (AAAA) protein. The results showed that the NLS mutant His_6–TFG–TEC (AAAA) protein co-precipitated specifically with GST–TFG–TEC (Figure 4A; top panel, lane 2), but not with GST alone (Figure 4A; top panel, lane 1). The three proteins were identified in the transfected cells by probing for GST (GST and GST–TFG–TEC; Figure 4A, middle panel) or the Xpress tag [His_6–TFG–TEC (AAAA); Figure 4A, lower panel]. These results show that the NLS mutant TFG–TEC (AAAA) protein can form a heterodimer with wild-type TFG–TEC *in vivo*.

The data in Figure 3(C) indicate that the DBD of TFG–TEC is capable of forming a heterodimer with TEC. To determine whether the NLS mutant form of TFG–TEC (DBD) was able to associate with wild-type TFG–TEC, GST pull-down assays were performed using the His_6–TFG–TEC protein. As shown in Figure 4(B) (top panel), the His_6–TFG–TEC protein interacted with both GST–DBD (AAAA) and GST–DBD, but not with GST alone. This indicates that the binding properties of the mutant DBD (AAAA) resemble those of the wild-type DBD within TFG–TEC. Aliquots of the GST-fusion proteins used in this assay were separated on SDS/PAGE (15 % gels) and visualized by Coomassie Blue staining to confirm that similar amounts of protein were used in the pull-down assays (Figure 4B; bottom panel).

The NLS mutant TFG–TEC (AAAA) protein traps wild-type TFG–TEC in the cytoplasm

Heterodimerization of wild-type TFG–TEC and the NLS mutant TFG–TEC proteins suggests that the NLS mutant [TFG–TEC (AAAA)] may affect the subcellular distribution of wild-type TFG–TEC protein. To investigate this, we co-transfected HEK-293T cells with mammalian expression vectors for EGFP-fused TFG–TEC (EGFP–TFG–TEC) and mCherry-fused NLS mutant TFG–TEC [mCherry–TFG–TEC (AAAA)]. In control HEK-293T cells not expressing the NLS mutant TFG–TEC (AAAA) protein, the EGFP-fused TFG–TEC protein was exclusively localized to the nucleus (Figure 5A, panels a–d). As expected, the NLS mutant TFG–TEC (AAAA) protein was localized to the cytoplasm in control HEK-293T cells (Figure 5A, panels e–h). Interestingly, Figure 5(A) (panels i–l) shows that, when

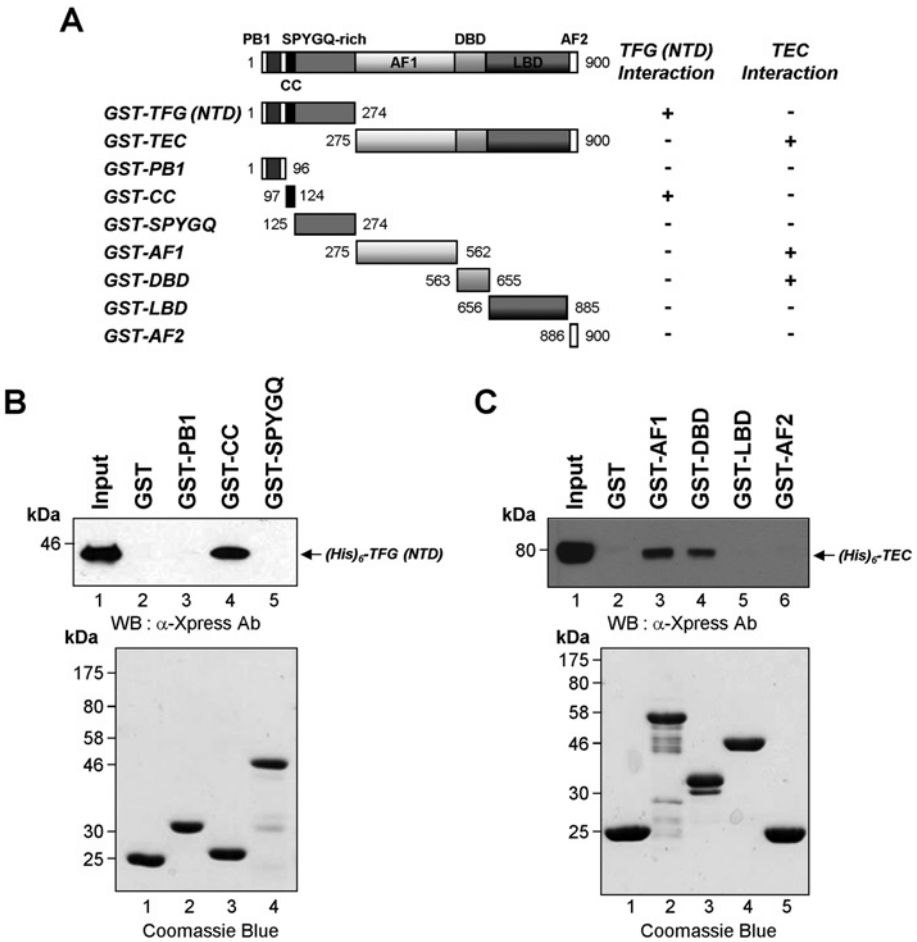

Figure 3 Mapping the domains responsible for TFG–TEC self-association

(**A**) Schematic representation of the GST–TFG–TEC fusion proteins and their ability to self-associate with TFG (NTD) or TEC fragments. Numbers refer to amino acid residues, and binding is indicated as + or -. (**B**) Binding of the TFG–TEC CC domain to the TFG (NTD). Recombinant His_6–TFG (NTD) protein was incubated with 2 μg of GST (lane 2), GST–PB1 (lane 3), GST–CC (lane 4) or GST–SPYGQ (lane 5) bound to glutathione–Sepharose beads. Aliquots of the input (2 %; lane 1) and the pellets (lanes 2–5) obtained from the GST pull-down assay were analysed on 12 % SDS/PAGE gels, and the bound proteins were detected by Western blotting with an anti-Xpress antibody (top panel). The positions of the molecular mass markers and His_6–TFG (NTD) are indicated. The relative abundance of the GST-fusion proteins was determined by separating them on SDS/PAGE (12 % gels) and visualizing them by Coomassie Blue staining (bottom panel). Lane 1, GST alone; lane 2, GST–PB1; lane 3, GST–CC; lane 4, GST–SPYGQ. Three independent experiments were performed, all of which gave similar results. Ab, antibody; WB, Western blotting. (**C**) Involvement of two independent domains of TFG–TEC in the interaction with TEC. Recombinant His_6-tagged TEC protein was incubated with 2 μg of GST (lane 2), GST–AF1 (lane 3), GST–DBD (lane 4), GST–LBD (lane 5) or GST–AF2 (lane 6) bound to glutathione–Sepharose beads. Aliquots of the input (2 %; lane 1) and the pellets (lanes 2–6) obtained from the GST pull-down assay were analysed on SDS/PAGE (8 % gels), and the bound proteins were detected by Western blotting with an anti-Xpress antibody (top panel). The positions of the molecular mass markers and His_6–TEC are indicated. The relative abundance of the GST-fusion proteins was determined by separating them on SDS/PAGE (12 % gels) and visualizing them by Coomassie Blue staining (bottom panel). Lane 1, GST alone; lane 2, GST–AF1; lane 3, GST–DBD; lane 4, GST–LBD; lane 5, GST–AF2. Three independent experiments were performed, all of which gave similar results. Molecular masses are indicated in kDa.

EGFP–TFG–TEC was co-expressed with the NLS mutant mCherry–TFG–TEC (AAAA), the wild-type TFG–TEC protein was expressed in both the cytoplasm and nucleus (Figure 5A, panel k, asterisks); however, wild-type TFG–TEC protein localized to the nucleus in cells not expressing the NLS mutant TFG–TEC (AAAA) (Figure 5A, panel k, arrowheads), suggesting that wild-type TFG–TEC was trapped in the cytoplasm by the NLS mutant TFG–TEC (AAAA) protein. Similar results were obtained in human C28/I2 chondrocyte cells. As shown in Figure 5(B), co-expression of the NLS mutant TFG–TEC (AAAA) protein trapped the wild-type TFG–TEC in the cytoplasm. Therefore we conclude that a proportion of wild-type TFG–TEC is retained within the cytoplasm upon co-expression of the NLS mutant TFG–TEC (AAAA) protein.

The NLS mutant TFG–TEC (AAAA) protein modulates TFG–TEC-dependent transactivation

To assess the consequences of heterodimerization between TFG–TEC and the NLS mutant TFG–TEC (AAAA) protein, we measured the effect of NLS mutant TFG–TEC (AAAA) protein expression on the levels of transcriptional activation mediated by wild-type TFG–TEC in HEK-293T cells. This was done by examining the expression of a luciferase-based reporter plasmid that was transfected into the cells along with pcDNA4-HisMaxB/TFG-TEC, either with or without co-transfection of pCMV-Tag2A/TFG-TEC (AAAA). The structures of the reporter plasmid and the expression vectors are shown in Figure 6(A). The introduction of TFG–TEC into HEK-293T cells activated

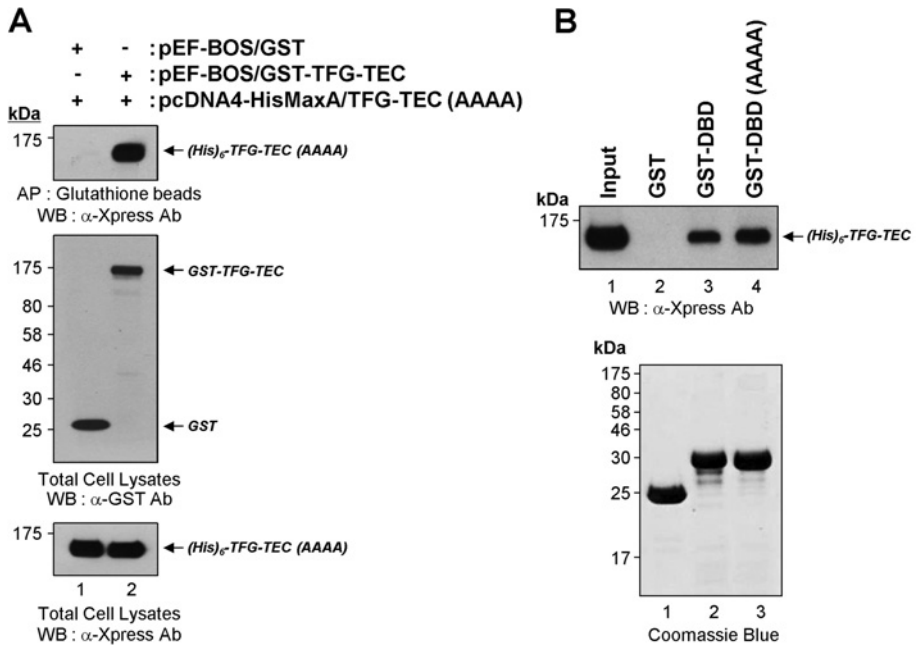

Figure 4 Association between the TFG–TEC (AAAA) mutant protein and wild-type TFG–TEC *in vivo*

(**A**) Physical association between TFG–TEC and an NLS mutant form of TFG–TEC (AAAA) *in vivo*. At 48 h after transfection of HEK-293T cells with 2.5 μg of pcDNA4-HisMaxA/TFG-TEC (AAAA) and 2.5 μg of either pEF-BOS/GST or pEF-BOS/GST-TFG-TEC, cell extracts were prepared as described in the Materials and methods section followed by affinity precipitation with glutathione–Sepharose beads. After separation by SDS/PAGE, the proteins were Western blotted with an anti-Xpress antibody or an anti-GST antibody. The transfected DNAs are indicated above the panel. The positions of the molecular mass markers are indicated on the left-hand side in kDa and the positions of His_6-tagged TFG–TEC (AAAA), GST and GST-tagged TFG–TEC are indicated by the arrows on the right-hand side. Three independent experiments gave similar results. Ab, antibody; AP, affinity precipitation; WB, Western blotting. (**B**) Wild-type TFG–TEC protein bound similarly to a wild-type DBD and the NLS mutant DBD (AAAA) protein. Recombinant His_6–TFG–TEC protein was incubated with 2 μg of GST (lane 2), GST–DBD (lane 3) or GST–DBD (AAAA) (lane 4) bound to glutathione–Sepharose beads. Aliquots of the input (2%; lane 1) and the pellets (lanes 2–4) obtained from the GST pull-down assay were analysed by SDS/PAGE (8% gels) and the bound proteins were detected by Western blotting with an anti-Xpress antibody (top panel). The positions of the molecular mass markers in kDa and His_6–TFG–TEC are indicated. The relative abundances of the GST-fusion proteins were determined by separation on SDS/PAGE (15% gels) and visualization by Coomassie Blue staining (bottom panel). Lane 1, GST alone; lane 2, GST–DBD; lane 3, GST–DBD (AAAA). Three independent experiments were performed, all of which gave similar results.

transcription (up to ~260-fold) of the p(B1a)^8-Luc, a reporter plasmid containing the TATA minimal promoter sequence and eight NBREs (nerve growth factor IB-response elements) [23], which drive the synthesis of *Renilla* luciferase (Figure 6B; top panel, bar 2). Interestingly, co-expression of the NLS mutant TFG–TEC (AAAA) protein inhibited wild-type TFG–TEC-mediated transactivation in a dose-dependent manner (Figure 6B; top panel, bars 3–6). These results indicate that the NLS mutant TFG–TEC (AAAA) protein inhibits TFG–TEC-mediated transactivation in HEK-293T cells. To control for cell-line-specific effects, we performed the same experiment in human C28/I2 chondrocytes and obtained similar results (Figure 6C, top panel). Therefore, we conclude that the NLS mutant TFG–TEC (AAAA) protein functions in a dominant-negative manner. Western blot analysis of cell extracts from transfected cells demonstrated modulation of TFG–TEC-dependent transactivation by the NLS mutant TFG–TEC (AAAA) was not due to differences in the amounts of TFG–TEC proteins (Figures 6B and 6C, second panels). In addition, Western blot analysis showed that higher amounts of the NLS mutant TFG–TEC (AAAA) protein were synthesized in response to increasing amounts of the transfected plasmids (Figures 6B and 6C, third panels). The EGFP plasmid served as an internal control for monitoring transfection efficiency (Figures 6B and 6C, bottom panels).

Next, to investigate whether ectopic co-expression of the NLS mutant TFG–TEC (AAAA) and wild-type TFG–TEC modulates the expression of endogenous downstream target genes for TFG–TEC *in vivo*, we transiently transfected HEK-293T cells with the TFG–TEC–EGFP and TFG–TEC (AAAA)–mCherry constructs. Consistent with previous reports [19,24], the expression of *Stat3*, *Eno3* and *Socs2* was up-regulated in HEK-293T cells transfected with TFG–TEC–EGFP (Figure 7A; lane 2). However, when the NLS mutant TFG–TEC (AAAA)–mCherry protein was co-expressed with wild-type TFG–TEC, the expression of *Stat3*, *Eno3* and *Socs2* was clearly down-regulated (Figure 7A; lane 3). HEK-293T cells expressing EGFP and mCherry were used as a control (Figure 7A; lane 1). Expression of the *Stat3*, *Eno3* and *Socs2* genes was unaffected in HEK-293T cells transfected with the EGFP and/or mCherry vector alone (results not shown). Similar results were obtained in human C28/I2 chondrocyte cells (Figure 7B).

To examine further the characteristics of HEK-293T cells co-expressing TFG–TEC and the NLS mutant TFG–TEC (AAAA) protein, we examined the expression of the *Stat3*, *Eno3* and *Socs2* genes using quantitative real-time PCR. As shown in Figure 7(C), expression of all three genes was up-regulated in HEK-293T cells expressing TFG–TEC–EGFP; however, these genes were down-regulated in HEK-293T cells co-expressing TFG–TEC–EGFP and TFG–TEC (AAAA)–mCherry. HEK-293T cells expressing EGFP and mCherry were used as a control. Expression of the *Stat3*, *Eno3* and *Socs2* genes was unaffected in HEK-293T cells transfected with the EGFP and/or mCherry vectors alone (results not shown). Similar results were obtained in human C28/I2 chondrocytes (Figure 7D). These results strongly suggest that the NLS mutant TFG–TEC (AAAA)

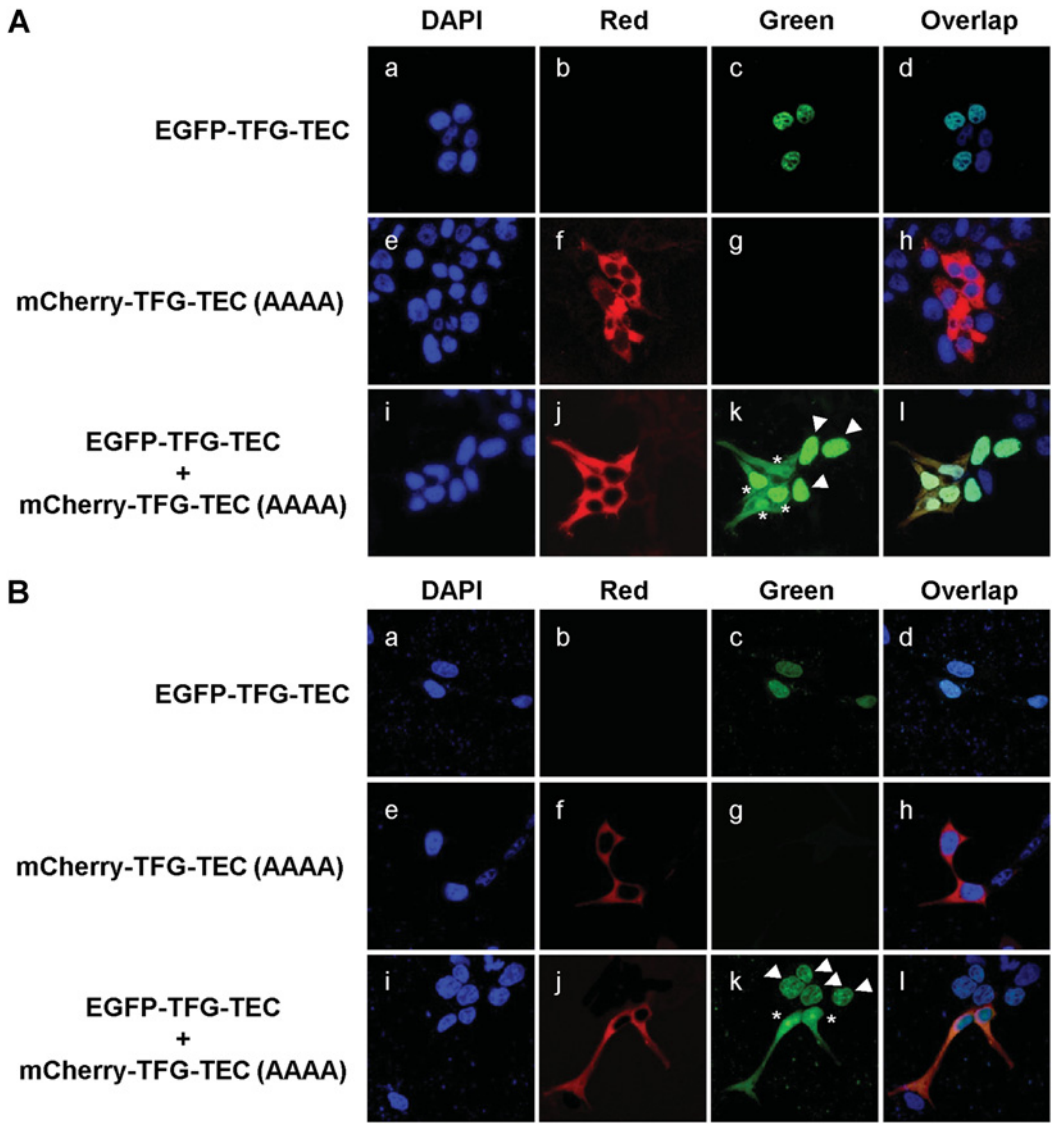

Figure 5 Nuclear trapping of wild-type TFG–TEC by the NLS mutant TFG–TEC (AAAA) protein in HEK-293T cells (A) and human C28/I2 chondrocytes (B)

HEK-293T or C28/I2 cells grown on coverslips were transfected with mammalian expression vectors encoding EGFP-tagged wild-type TFG–TEC (green) or mCherry-tagged NLS mutant TFG–TEC (AAAA) (red) proteins. Transiently transfected cells were fixed with an acetone/methanol mixture and the subcellular distribution of wild-type TFG–TEC or the NLS mutant TFG–TEC (AAAA) protein was examined under a confocal laser-scanning microscope (Leica TCS SPE). Cell nuclei were stained with DAPI. Merged images are also shown. Three independent experiments were performed, all of which gave similar results. See the text for more information. Magnification: ×400.

protein down-regulates TFG–TEC-mediated transactivation, and functions as a dominant-negative regulator of the wild-type TFG–TEC protein both *in vitro* and *in vivo*.

DISCUSSION

In the present study we present a comprehensive analysis of a TFG–TEC chimaeric molecule generated by a chromosomal translocation in human EMCs. Targeting TFG–TEC may lead to the development of novel therapeutic strategies for this aggressive cancer, therefore understanding the biochemical properties of TFG–TEC may help to identify the mechanisms underlying TFG–TEC-mediated malignancy. The present study shows that TFG–TEC self-associates both *in vitro* and *in vivo*, and that TFG–TEC-mediated transcriptional activation can be antagonized by an NLS mutant TFG–TEC (AAAA) protein. Taken together, this information suggests that the biological activity of the TFG–TEC chimaeric protein can be regulated by its dominant-negative form. The results reported in the present paper explore the functional regulation of the TFG–TEC oncoprotein.

The NLS mutant TFG–TEC (AAAA) protein effectively impaired the activity of wild-type TFG–TEC (Figures 6 and 7), therefore it was necessary to examine the mechanisms underlying this inhibition. As the NLS mutant TFG–TEC (AAAA) protein is a cytoplasmic protein, it may inactivate the TFG–TEC oncoprotein by causing its mislocalization within the cell. Our initial approach involved characterizing the association between wild-type TFG–TEC and the NLS mutant TFG–TEC (AAAA) protein. To this end, we determined whether the NLS mutant TFG–TEC (AAAA) protein was able

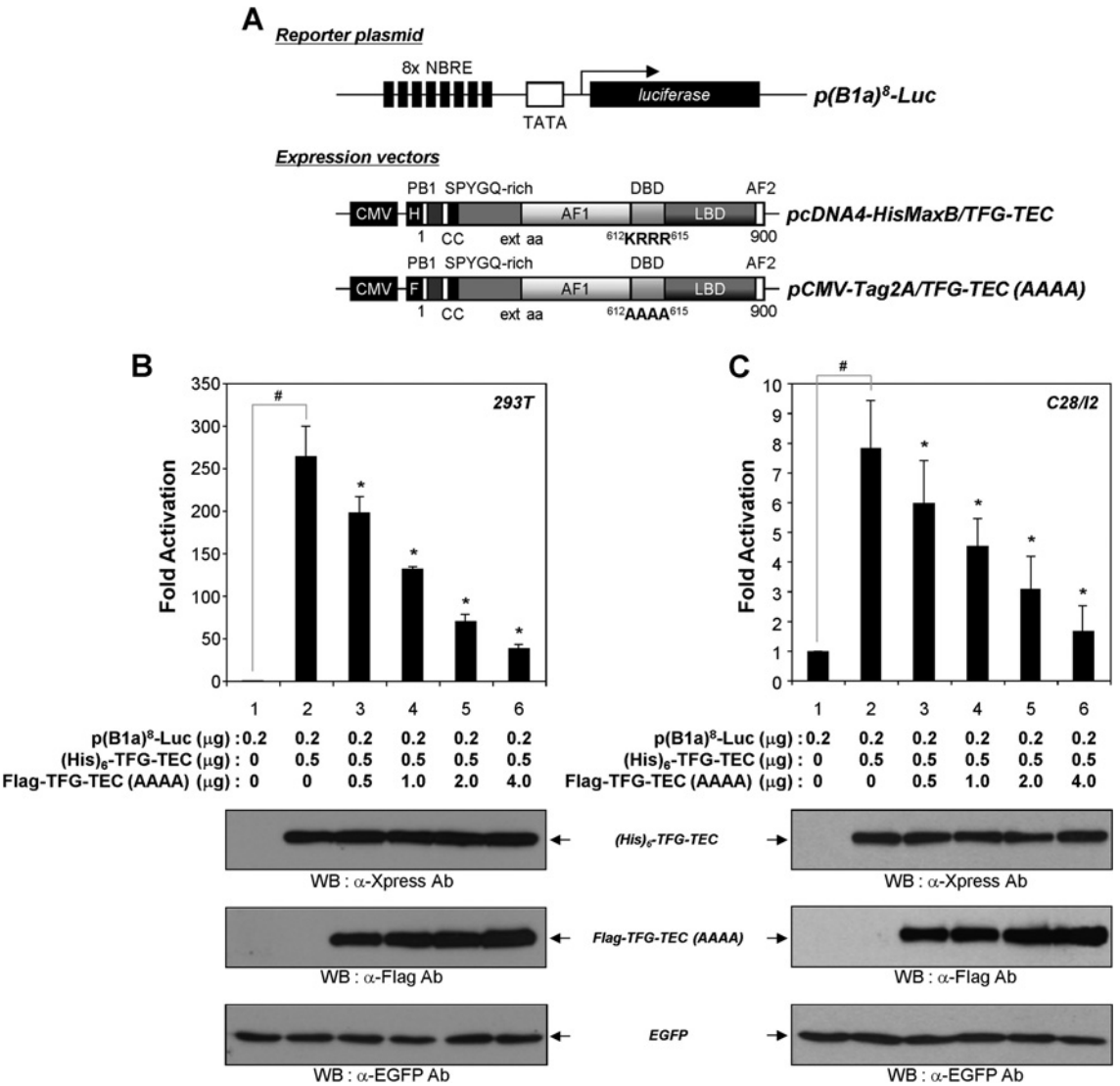

Figure 6 The NLS mutant TFG–TEC (AAAA) protein interferes with TFG–TEC-mediated transactivation

(**A**) Schematic representation of the reporter and expression plasmids used in the present study. The p(B1a)^8-Luc reporter plasmid contains eight NBREs upstream of a basal promoter–luciferase gene construct. The eight TFG–TEC recognition sites are indicated by solid bars, the TATA box is represented by an open box and the luciferase gene is indicated by a solid box. The expression vectors driving the production of TFG–TEC or TFG–TEC (AAAA) are also shown. The positions of the first and last amino acids are indicated below each construct. AF1, N-terminal transactivation domain; AF2, C-terminal transactivation domain; CMV, cytomegalovirus promoter; ext aa, extra amino acid sequence; F, FLAG-tag; H, His_6 tag. (**B** and **C**) The NLS mutant TFG–TEC (AAAA) protein inhibits TFG–TEC-mediated transactivation in HEK-293T cells (**B**) and human C28/I2 chondrocytes (**C**). HEK-293T or C28/I2 cells were co-transfected with 0.5 μg of TFG–TEC and increasing amounts (0–4 μg) of the NLS mutant TGF-TEC (AAAA) protein. For all reactions, the total amount of transfected DNA was normalized against the amount of empty vectors. After 48 h, the cells were harvested and luciferase assays were performed. The means $\pm$ S.E.M. from representative duplicate experiments are presented. Statistical significance (P value) was determined with an unpaired t test. #$P < 0.001$ compared with vector control; *$P < 0.01$ compared with wild-type TFG–TEC alone (top panels). Extracts for luciferase assays were resolved by SDS/PAGE (8% gels for top and middle panels, and 15% gels for bottom panels), transferred on to a PVDF membrane, and immunoblotted with anti-Xpress (second panels), anti-FLAG (M2, Sigma–Aldrich; third panels) and anti-EGFP (bottom panels) antibodies. Three independent experiments were performed, all of which gave similar results. Ab, antibody; WB, Western blot.

to disrupt the nuclear localization of wild-type TFG–TEC, a characteristic required for TFG–TEC-mediated transcriptional transactivation. First, to examine the association between the wild-type and NLS mutant TFG–TECs, we performed affinity precipitation assays followed by Western blot analysis to detect the wild-type TFG–TEC and NLS mutant TFG–TEC (AAAA) proteins. Because transcriptional transactivation by TFG–TEC requires that TFG–TEC is localized to the nucleus [19], we next examined whether the NLS mutant TFG–TEC (AAAA) protein altered the cellular localization of TFG–TEC in transfected HEK-293T and human C28/I2 chondrocytes. As expected, wild-type TFG–TEC localized predominantly to the nucleus in HEK-293T cells and human C28/I2 chondrocytes when expressed in the absence of the NLS mutant TFG–TEC (AAAA) protein. By contrast, the NLS mutant TFG–TEC (AAAA) protein remained predominantly in the cytoplasm when expressed in the absence of wild-type TFG–TEC (Figure 5). When TFG–TEC and the NLS mutant TFG–TEC (AAAA) protein were co-expressed, the NLS mutant localized to the cytoplasm; surprisingly, however, wild-type TFG–TEC was present in both the nucleus and cytoplasm (Figure 5). This suggests that the NLS mutant TFG–TEC (AAAA) protein was able to shift the

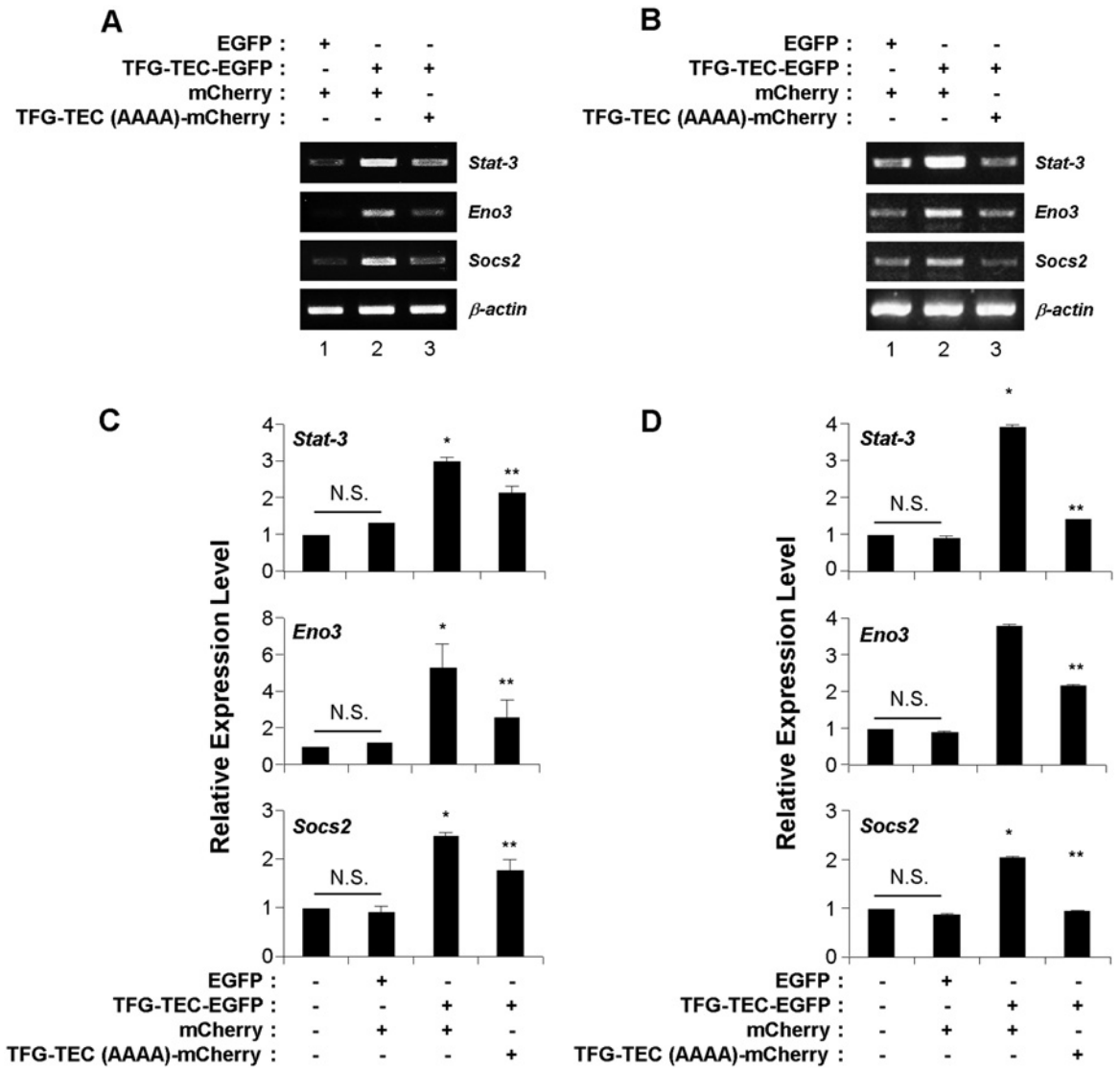

Figure 7 The NLS mutant TFG–TEC (AAAA) protein suppresses the transactivation potential of wild-type TFG–TEC *in vivo*

(**A** and **B**) TFG–TEC (AAAA) interferes with the induction of TFG–TEC downstream target genes in HEK-293T cells (**A**) and human C28/I2 chondrocytes (**B**). HEK-293T or C28/I2 cells were co-transfected with expression vectors encoding EGFP, TFG–TEC–EGFP, mCherry or TFG–TEC (AAAA)–mCherry (indicated above the panels). EGFP-positive and mCherry-positive transfected cells were isolated by FACS. RT–PCR analysis of *Stat3*, *Eno3* and *Socs2* mRNA expression was performed in HEK-293T cells (**A**) and C28/I2 chondrocyte cells (**B**) expressing EGFP and mCherry, TFG–TEC–EGFP and mCherry or TFG–TEC–EGFP and TFG–TEC (AAAA)–mCherry proteins. β-Actin was used for normalization. Following amplification, an aliquot of each product was analysed by staining the gel with ethidium bromide. The vectors pcDNA3-TFG-TEC-EGFP and pcDNA3-TFG-TEC (AAAA)-mCherry were used to express TFG–TEC or TFG–TEC (AAAA) fused to EGFP or mCherry respectively. pcDNA3-EGFP or pcDNA3-mCherry expression vectors were used as controls. The transiently transfected cell lines (from which the input RNAs used in the RT reactions were derived) are shown above the panel. Three independent experiments were performed, all of which gave similar results. (**C** and **D**) Quantitative real-time PCR analyses of the expression of putative TFG–TEC downstream target genes in HEK-293T (**C**) and C18/I2 (**D**) cells. HEK-293T and C28/I2 cells were analysed for their expression of *Stat3*, *Eno3* and *Socs2* mRNA as described in the Materials and methods section. *HPRT* was used as a control to normalize the quantitative real-time PCR results. Each transfection was performed at least three times. The results are the means $\pm$ S.E.M. and are calculated relative to the expression of *Stat3*, *Eno3* or *Socs2* in EGFP- and mCherry-transfected cells (which was set at 1). Statistical significance (*P* value) was determined with an unpaired *t* test. $^{*}P < 0.01$ compared with vector control; $^{**}P < 0.01$ compared with wild-type TFG–TEC alone. N.S., not significant.

localization of the wild-type TFG–TEC from the nucleus to the cytoplasm. Thus the NLS mutant TFG–TEC (AAAA) protein appears to form a heterodimer with the wild-type protein to yield non-productive complexes. The net result is antagonism of wild-type TFG–TEC activity via a dominant-negative mechanism.

The mixed pattern of subcellular localization in Figure 5 suggests that the inhibitory effect of the NLS-mutant TFG–TEC (AAAA) was not complete. However, this mixed pattern of wild-type TFG–TEC localization, both in the cytoplasm and in the nucleus, is consistent with the predicted association properties of these proteins. When the NLS-mutant TFG–TEC (AAAA) was co-expressed with wild-type TFG–TEC in the same cell, a time-dependent association between these two proteins occurs *in vivo*. As shown in Figures 1 and 4, the wild-type TFG–TEC protein associated with either TFG–TEC (AAAA) or TFG–TEC protein. Consequently, three protein complexes, i.e. wild-type homodimers, wild-type-mutant heterodimers and mutant homodimers, would be expected to exist in these cells. Among these complexes, heterodimerization of the NLS-mutant TFG–TEC with wild-type TFG–TEC would have resulted in

trapping of the wild-type TFG–TEC protein in the cytoplasm (Figure 5); however, homodimerization of wild-type TFG–TEC proteins would not have affected their nuclear localization. For this reason, it seems reasonable to speculate that the mixed pattern of subcellular localization was not due to the incomplete inhibitory effect of the NLS-mutant TFG–TEC *in vivo*, but rather to the dimerization properties of these proteins. In addition, it would be interesting to investigate the thermodynamics and kinetic properties of the association between the wild-type TFG–TEC and the NLS-mutant TFG–TEC for the development of a therapy against aggressive EMCs.

The N-terminal fragment of the TFG polypeptide shows strong similarities to the N-terminal fragments of the EWS, TLS (translated in liposarcoma) and $hTAF_{II}68$ proteins [8,11]. The *EWS*, *TLS* and *$hTAF_{II}68$* genes, which were originally identified as the N-terminal portions of translocation-generated fusion genes in human cancers, encode a putative RNA-binding domain and three glycine-, arginine- and proline-rich motifs [25]. In contrast with that of EWS-, TLS- and $hTAF_{II}68$-fusion proteins, the regulation of TFG–TEC remains poorly understood. During the course of the present study, we noticed that the TFG–TEC chimaeric protein could self-associate. Therefore, our initial experiments used GST pull-down and *in vivo* affinity precipitation assays to study the potential of TFG–TEC to form homodimers. Interestingly, we found that three independent domains, CC, AF1 and DBD, were involved in the self-association of TFG–TEC (Figure 3). Because the biological functions of some cellular proteins are regulated by their ability to self-associate, it would be interesting to examine whether these independent interacting domains are also important for TFG–TEC function.

In a previous study, we showed that TFG–TEC is a nuclear protein that binds DNA with a sequence specificity identical to that of the parental TEC protein [19]. Therefore we investigated the molecular mechanism underlying TFG–TEC-mediated tumorigenesis in human EMCs. We found that TFG–TEC shows increased transcriptional activation potential, although it contains the complete amino acid sequence for TEC. This indicates that the N-terminal portion of TFG–TEC may provide additional transactivation properties. Consistent with this, the TFG (NTD) region functioned as a transcription activation domain when coupled to a GAL4 DBD. TFG (NTD) also self-associates (Figure 2) and the CC domain within TFG (NTD) is required for this (Figure 3); therefore, it would be interesting to examine whether CC domain-mediated TFG (NTD) self-association is important for its transactivation properties.

In summary, the present study identified a novel NLS mutant of TFG–TEC and demonstrated how it regulates the cellular localization and transcriptional activity of wild-type TFG–TEC. Although we previously reported that: (i) TFG–TEC is a nuclear protein that binds DNA with a sequence specificity identical to that of the parental TEC protein; (ii) the fusion gene encodes a transactivator that is more potent than TEC; and (iii) the functions of TFG–TEC may be necessary for tumorigenesis in human EMCs [19], the functional regulation of this protein is still unknown. Therefore understanding the mechanisms that regulate TFG–TEC may lead to the development of novel therapeutic strategies and targets for the treatment of aggressive EMCs harbouring characteristic t(3;9) translocation.

AUTHOR CONTRIBUTION

Bobae Lim and Ah-young Kim conceived and designed the project, collected and assembled the data, and interpreted the data. Hee Jung Jun collected and assembled the data. Jungho Kim conceived and designed the project, collected and assembled the data, analysed and interpreted the data, provided financial support and wrote the paper.

ACKNOWLEDGEMENTS

We thank Dr Yves Labelle (Laval University Faculty of Medicine, Quebec City, QC, Canada) for providing the p(B1a)8-Luc reporter plasmid and Dr Mary B. Goldring (Hospital for Special Surgery and Cornell Medical College, New York, NY, U.S.A.) for providing the human C28/I2 juvenile costal chondrocyte cells.

FUNDING

This work was supported by the National Research Foundation of Korea (NRF) [grant number 2013R1A1A2009478], the Bio and Medical Technology Development Programme [grant number 2012M3A9B4028763], the Priority Research Centers Program [grant number 2009-0093822] through the National Research Foundation of Korea funded by the Ministry of Education and the Ministry of Science, Information, Communication, Technology and Future Planning, and by the Sogang Research Frontier Program (SRF) [grant number 2012-14003] from Sogang University. A.Y.K., B.L. and H.J.J. were recipients of a research fellowship from the Ministry of Education and Human Resources Development [number BK21].

REFERENCES

1 Clark, J., Benjamin, H., Gill, S., Sidhar, S., Goodwin, G., Crew, J., Gusterson, B. A., Shipley, J. and Cooper, C. S. (1996) Fusion of the EWS gene to CHN, a member of the steroid/thyroid receptor gene superfamily, in a human myxoid chondrosarcoma. Oncogene **12**, 229–235

2 Labelle, Y., Bussieres, J., Courjal, F. and Goldring, M. B. (1999) The EWS/TEC fusion protein encoded by the t(9;22) chromosomal translocation in human chondrosarcomas is a highly potent transcriptional activator. Oncogene **18**, 3303–3308

3 Labelle, Y., Zucman, J., Stenman, G., Kindblom, L. G., Knight, J., Turc-Carel, C., Dockhorn-Dworniczak, B., Mandahl, N., Desmaze, C., Peter, M. et al. (1995) Oncogenic conversion of a novel orphan nuclear receptor by chromosome translocation. Hum. Mol. Genet. **4**, 2219–2226

4 Sjogren, H., Meis-Kindblom, J., Kindblom, L. G., Aman, P. and Stenman, G. (1999) Fusion of the EWS-related gene TAF2N to TEC in extraskeletal myxoid chondrosarcoma. Cancer Res. **59**, 5064–5067

5 Attwooll, C., Tariq, M., Harris, M., Coyne, J. D., Telford, N. and Varley, J. M. (1999) Identification of a novel fusion gene involving hTAFII68 and CHN from a t(9;17)(q22;q11.2) translocation in an extraskeletal myxoid chondrosarcoma. Oncogene **18**, 7599–7601

6 Panagopoulos, I., Mencinger, M., Dietrich, C. U., Bjerkehagen, B., Saeter, G., Mertens, F., Mandahl, N. and Heim, S. (1999) Fusion of the RBP56 and CHN genes in extraskeletal myxoid chondrosarcomas with translocation t(9;17)(q22;q11). Oncogene **18**, 7594–7598

7 Sjogren, H., Wedell, B., Meis-Kindblom, J. M., Kindblom, L. G., Stenman, G. and Kindblom, J. M. (2000) Fusion of the NH_2-terminal domain of the basic helix-loop-helix protein TCF12 to TEC in extraskeletal myxoid chondrosarcoma with translocation t(9;15)(q22;q21). Cancer Res. **60**, 6832–6835

8 Hisaoka, M., Ishida, T., Imamura, T. and Hashimoto, H. (2004) TFG is a novel fusion partner of NOR1 in extraskeletal myxoid chondrosarcoma. Genes, Chromosomes Cancer **40**, 325–328

9 Greco, A., Mariani, C., Miranda, C., Lupas, A., Pagliardini, S., Pomati, M. and Pierotti, M. A. (1995) The DNA rearrangement that generates the TRK-T3 oncogene involves a novel gene on chromosome 3 whose product has a potential coiled-coil domain. Mol. Cell. Biol. **15**, 6118–6127

10 Hernandez, L., Pinyol, M., Hernandez, S., Bea, S., Pulford, K., Rosenwald, A., Lamant, L., Falini, B., Ott, G., Mason, D. Y. et al. (1999) TRK-fused gene (TFG) is a new partner of ALK in anaplastic large cell lymphoma producing two structurally different TFG-ALK translocations. Blood **94**, 3265–3268

11 Mencinger, M., Panagopoulos, I., Andreasson, P., Lassen, C., Mitelman, F. and Aman, P. (1997) Characterization and chromosomal mapping of the human TFG gene involved in thyroid carcinoma. Genomics **41**, 327–331

12 Miranda, C., Roccato, E., Raho, G., Pagliardini, S., Pierotti, M. A. and Greco, A. (2006) The TFG protein, involved in oncogenic rearrangements, interacts with TANK and NEMO, two proteins involved in the NF-κB pathway. J. Cell. Physiol. **208**, 154–160

13 Ohkura, N., Hijikuro, M., Yamamoto, A. and Miki, K. (1994) Molecular cloning of a novel thyroid/steroid receptor superfamily gene from cultured rat neuronal cells. Biochem. Biophys. Res. Commun. **205**, 1959–1965

14 Hedvat, C. V. and Irving, S. G. (1995) The isolation and characterization of MINOR, a novel mitogen-inducible nuclear orphan receptor. Mol. Endocrinol. **9**, 1692–1700

15 Maltais, A. and Labelle, Y. (2000) Structure and expression of the mouse gene encoding the orphan nuclear receptor TEC. DNA Cell Biol. **19**, 121–130
16 Cheng, L. E., Chan, F. K., Cado, D. and Winoto, A. (1997) Functional redundancy of the Nur77 and Nor-1 orphan steroid receptors in T-cell apoptosis. EMBO J. **16**, 1865–1875
17 Sambrook, J. and Russell, D. W. (2001) Molecular Cloning: a Laboratory Manual. Cold Spring Harbor Laboratory Press, New York
18 Lee, J., Kim, H. K., Han, Y. M. and Kim, J. (2008) Pyruvate kinase isozyme type M2 (PKM2) interacts and cooperates with Oct-4 in regulating transcription. Int. J. Biochem. Cell Biol. **40**, 1043–1054
19 Lim, B., Jun, H. J., Kim, A. Y., Kim, S., Choi, J. and Kim, J. (2012) The TFG-TEC fusion gene created by the t(3;9) translocation in human extraskeletal myxoid chondrosarcomas encodes a more potent transcriptional activator than TEC. Carcinogenesis **33**, 1450–1458
20 Lee, H. J., Kim, S., Pelletier, J. and Kim, J. (2004) Stimulation of hTAFII68 (NTD)-mediated transactivation by v-Src. FEBS Lett. **564**, 188–198
21 Lee, J., Kim, H. K., Rho, J. Y., Han, Y. M. and Kim, J. (2006) The human OCT-4 isoforms differ in their ability to confer self-renewal. J. Biol. Chem. **281**, 33554–33565
22 Lee, J., Rhee, B. K., Bae, G. Y., Han, Y. M. and Kim, J. (2005) Stimulation of Oct-4 activity by Ewing's sarcoma protein. Stem Cells **23**, 738–751
23 Wilson, T. E., Fahrner, T. J., Johnston, M. and Milbrandt, J. (1991) Identification of the DNA binding site for NGFI-B by genetic selection in yeast. Science **252**, 1296–1300
24 Ohkura, N., Nagamura, Y. and Tsukada, T. (2008) Differential transactivation by orphan nuclear receptor NOR1 and its fusion gene product EWS/NOR1: possible involvement of poly(ADP-ribose) polymerase I, PARP-1. J. Cell. Biochem. **105**, 785–800
25 Kim, J. and Pelletier, J. (1999) Molecular genetics of chromosome translocations involving EWS and related family members. Physiol. Genomics **1**, 127–138

Received 8 April 2013/9 September 2013; accepted 30 September 2013
Published as BJ Immediate Publication 30 September 2013, doi:10.1042/BJ20130486